

# Wogonin Alleviates Kidney Tubular Epithelial Injury in Diabetic Nephropathy by Inhibiting PI3K/Akt/NF- $\kappa$ B Signaling Pathways

Lei Lei <sup>1</sup>  
Jing Zhao<sup>1</sup>  
Xue-Qi Liu <sup>1</sup>  
Juan Chen<sup>1</sup>  
Xiang-Ming Qi<sup>1</sup>  
Ling-Ling Xia<sup>2</sup>  
Yong-Gui Wu<sup>1</sup>

<sup>1</sup>Department of Nephropathy, the First Affiliated Hospital of Anhui Medical University, Hefei, Anhui, 230022, People's Republic of China; <sup>2</sup>Department of Infectious Disease, the First Affiliated Hospital of Anhui Medical University, Hefei, Anhui, 230022, People's Republic of China

Correspondence: Ling-Ling Xia  
Department of Infectious Disease, The First Affiliated Hospital of Anhui Medical University, Hefei, Anhui, People's Republic of China  
Tel +86 0551 6292 2450  
Email 13966684365@163.com

Yong-Gui Wu  
Department of Nephropathy, The First Affiliated Hospital of Anhui Medical University, Hefei, Anhui, People's Republic of China  
Tel +86 0551 6292 2111  
Email wuyonggui@medmail.com.cn

**Introduction:** Kidney tubular epithelial injury is one of the key factors in the progression of diabetic nephropathy (DN). Wogonin is a kind of flavonoid, which has many pharmacological effects, such as anti-inflammation, anti-oxidation and anti-fibrosis. However, the effect of wogonin in renal tubular epithelial cells during DN is still unknown.

**Materials and Methods:** STZ-induced diabetic mice were given doses of wogonin (10, 20, and 40 mg/kg) by intragastric administration for 16 weeks. The metabolic indexes from blood and urine and pathological damage of renal tubules in mice were evaluated. Human tubular epithelial cells (HK-2) were cultured in high glucose (HG) condition containing wogonin (2 $\mu$ M, 4 $\mu$ M, 8 $\mu$ M) for 24 h. Tubular epithelial cell inflammation and autophagic dysfunction both in vivo and in vitro were assessed by Western blot, qRT-PCR, IHC, and IF analyses.

**Results:** The treatment of wogonin attenuated urinary albumin and histopathological damage in tubulointerstitium of diabetic mice. We also found that wogonin down-regulated the expression of pro-inflammatory cytokines and autophagic dysfunction in vivo and in vitro. Molecular docking and Cellular Thermal Shift Assay (CETSA) results revealed that mechanistically phosphoinositide 3-kinase (PI3K) was the target of wogonin. We then found that inhibiting PI3K eliminated the protective effect of wogonin. Wogonin regulated autophagy and inflammation via targeting PI3K, the important connection point of PI3K/Akt/NF- $\kappa$ B signaling pathway.

**Conclusion:** Our study is the first to demonstrate the novel role of wogonin in mitigating tubulointerstitial fibrosis and renal tubular cell injury via regulating PI3K/Akt/NF- $\kappa$ B signaling pathway-mediated autophagy and inflammation. Wogonin might be a latent remedial drug against tubular epithelial injury in DN by targeting PI3K.

**Keywords:** diabetic nephropathy, tubular epithelial cell, wogonin, inflammation, autophagy, PI3K/Akt/NF- $\kappa$ B pathway

## Introduction

Diabetic nephropathy (DN) is one of the most important complications of diabetic patients, and it is also the main cause of end-stage renal disease (ESRD).<sup>1</sup> Studies have shown that renal tubular cells were already damaged in early DN, and chronic exposure to high blood glucose levels lead to tubulointerstitial changes in overt DN.<sup>2,3</sup> Clinically, a decrease in glomerular filtration rate correlates better with tubulointerstitial injury than with glomerular damage.<sup>4</sup> The continuous decline in renal function is closely related to the progressive accumulation of extracellular matrix (ECM) proteins.<sup>5</sup> Under high glucose (HG) condition, renal tubular epithelial cells show phenotypic and functional

changes, which convert from tubular structure to interstitial.<sup>6</sup> Excessive matrix disperses between and around the tubular structures. With the progression of disease, it evolved into the accumulation of ECM of tubulointerstitial fibrosis, which ultimately caused irreversible injury to renal structure.<sup>7</sup>

Wogonin (5, 7-dihydroxy-8-methoxyflavone), a flavonoid, has many pharmacological effects such as anti-inflammation, anti-oxidation and anti-fibrosis.<sup>8,9</sup> Studies have shown that wogonin can inhibit the level of  $\alpha$ -smooth muscle actin ( $\alpha$ -SMA) and collagen I (Col-I) induced by TGF- $\beta$ 1, thereby inhibiting the fibrosis of renal tubular epithelial cells.<sup>10</sup> Furthermore, wogonin can effectively inhibit inflammation and fibrosis in HG-induced mesangial cells.<sup>11</sup> Wogonin enhances oxaliplatin-induced gastric cancer cell death by promoting excessive autophagy.<sup>12</sup> However, the role of wogonin in renal tubular epithelial cells during DN is unknown.

Long-term chronic inflammation is a critical factor in the development of DN.<sup>13</sup> Recent research results have shown that the expression of pro-inflammatory cytokines in diabetic patients is increased.<sup>14–16</sup> At the same time, the urinary albumin in DN patients also stimulated proximal tubule cells to produce a series of inflammation response, leading to renal tubular cell damage.<sup>17,18</sup>

Autophagy is an important degradation mechanism to degrade the damaged organelles and proteins to maintain cell homeostasis under diverse stress conditions.<sup>19</sup> More and more studies have shown that autophagic dysfunction can make disease worse in renal disease.<sup>20–23</sup> Cytokines released under inflammatory stress condition may contribute to dysfunction of tubular autophagy in diabetes and decrease autophagic clearance, which leads to accumulation of damaged proteins that aggravate kidney damage.<sup>24–26</sup> Studies have shown that autophagy is significantly inhibited in STZ-induced diabetic mice, which is manifested by accumulation of autophagy substrate P62/SQSTM1 caused renal tubular cell damage.<sup>27</sup> Therefore, regulating autophagic activity plays a critical role in DN.

Now, our research showed that protective effect of wogonin on renal tubular epithelial cells in diabetic mice, and firstly found that wogonin regulated autophagy and inflammation via targeting phosphoinositide 3-kinase (PI3K), the important connection point of PI3K/Akt/NF- $\kappa$ B signaling pathway. Moreover, we preliminarily confirmed that wogonin may bind to PI3K through molecular docking and CETSA. When cells were pre-treated with PI3K inhibitor (PI3Ki), LY294002, it was further determined that wogonin was unable to reverse HG-induced cell injury after inhibiting PI3K. Hence, we demonstrated

that wogonin functioned through PI3K-dependent pathways. Together, wogonin might be a latent therapeutic drug against DN by targeting PI3K.

## Materials and Methods

### Drugs and Reagents

Wogonin was acquired from Aladdin Biology Technology Institute (W101155, CAS 632–85-9, Shanghai, China). Streptozotocin (STZ) was obtained from Sigma-Aldrich (Saint Louis, MO, USA). PI3K inhibitor LY294002 was acquired from MedChem Express (Princeton, USA). DMEM was obtained from Gibco (Gibco, CA). The NF- $\kappa$ B p65 and p-NF- $\kappa$ B p65 antibody, anti-LC3 antibody, anti-P62 antibody, anti-Beclin1 antibody, anti-Akt and anti-p-Akt were obtained from Cell Signaling Technology (Danvers, MA, USA). The antibodies anti-KIM-1, anti-Atg7 and anti-fibronectin (FN) were obtained from Abcam (Cambridge, USA). Anti- $\alpha$ -SMA and anti-E-cadherin antibodies were acquired from Proteintech (Wuhan, China). Anti-Col-I antibody was acquired from Bioss (Shanghai, China). Anti-PI3K and Anti-p-PI3K were obtained from Affinity Biosciences (Affinity, USA). Periodic acid-Schiff (PAS), creatinine (CRE), blood urea nitrogen (BUN) kits were purchased from Jiancheng Biology Technology Institute (Nanjing, China). Albumin ELISA kit was acquired from Abcam (Cambridge, USA).

### STZ-Induced Diabetic Mice Models

Weight-matched C57/BL male mice (6–8 weeks) were obtained from the Experimental Animal Centre, Anhui Medical University. Mice were confirmed to be diabetic mice models after intraperitoneal injection of 50 mg/kg STZ for 5 days. The mice were kept in an animal facility with a 12 h light/dark cycle, allowing free access to normal water and food in a room with a steady temperature of 22°C  $\pm$ 2°C and a humidity of 60%. The mice were randomly divided into six groups (n = 6–8): normal control (NC), normal control + wogonin (40 mg/kg, Wog), diabetes group (DM), DM + wogonin group (10 mg/kg, 20 mg/kg, 40 mg/kg). The DM+Wog groups and the Wog group were received with wogonin every other day for 16 weeks. DM and NC groups were given with the same amount of saline. Animal experiments were conducted in accordance with “Guide for the Care and Use of Laboratory Animals” (National Institutes of Health Publication No. 85–23, revised 1996). Ethical approval and experiments were approved by Anhui Medical University Ethics Committee (approval No. 20200066).

## Biochemical and Physical Assay

Fasting blood glucose levels were measured by an Accu-Chek glucose meter (Roche diagnostics device). The 24 h urinary albumin levels, CRE and BUN were detected with kits obtained from the Jiancheng Biology Technology Institute (Nanjing, China). Each mouse's body weight and kidney weight were measured.

## Kidney Histology

Renal tissue was fixed in 4% paraformaldehyde for 24 h. Renal tissue sections from paraffin-embedded kidneys cut into 4  $\mu$ m thickness. After deparaffinization, periodic acid-Schiff (PAS) and Masson's trichrome were performed to estimate renal morphology, glycogen accumulation and collagen accumulation. Photographs were taken by microscope (Zeiss AX10 microscope, Carl Zeiss Canada Ltd, Canada) at  $\times$ 400 magnification. The staining kits were purchased from Beijing Solarbio Science & Technology Co., Ltd. Sections were visualized after counterstained with hematoxylin under a microscope.

## Immunohistochemistry Assay

The samples were soaked in xylene and graded ethanol. The antigens were exposed by heat-induced epitope retrieval. Renal tissue sections were blocked with goat serum at 37°C for 45 min and incubated with antibodies against TNF- $\alpha$ , Col-I, FN, E-cadherin and  $\alpha$ -SMA, at 4°C overnight. Subsequently, secondary antibodies for 30 min at 37°C. Sections were visualized after counterstained with hematoxylin under a microscope.

## Cell Culture

HK-2 cells were supplied by Professor Huiyao Lan from the Chinese University of Hong Kong. HK-2 cells were cultured in low glucose (5.5 mM glucose) DMEM containing 10% FBS and conditions were maintained at 37°C, 5% CO<sub>2</sub>. Then, HK-2 cells were cultured in low glucose (5.5 mM glucose, LG), mannitol (5.5 mM glucose+24.5 mM mannitol, MG), low glucose with wogonin (LG+8  $\mu$ M, Wog), high glucose (30 mM glucose, HG), and high glucose with wogonin (2  $\mu$ M, 4  $\mu$ M, 8  $\mu$ M) mediums for 24 h. LG and MG mediums were used as controls. Cell experiment has been approved by Anhui Medical University Ethics Committee (approval No. 20200018).

## MTT Assay

HK-2 cells were seeded in 96-well plates and cultured in different concentrations of wogonin for 24 h and then added

in high glucose DMEM (30 mM glucose) for 24 h. Subsequently, put 5 mg/mL of MTT solution in each well and incubated for 4 h at 37°C. Finally, the optical density (OD) was measured by a microplate reader (Multiskan MK3, Thermo, USA) at 550 nm.

## PI3K Inhibitor

The suitable concentration of PI3Ki concentration used in study was determined by MTT and Western blot. Then, HK-2 cells were cultured in low glucose (5.5 mM glucose), high glucose (30 mM glucose, HG) and high glucose with wogonin (2  $\mu$ M, 4  $\mu$ M, 8  $\mu$ M, HG+Wog) mediums with or without PI3Ki for 24 h.

## Transmission Electron Microscopy

The cells were prefixed with 2.5% glutaraldehyde for 72 h and 1% osmium tetroxide for 1 h. Polymerization was accomplished in gelatin capsules at 60°C for 48 h and observed under a transmission electron microscope (H-7700166 Tokyo, Japan).

## ELISA Assay

The pro-inflammatory cytokines IL-1 $\beta$ , TNF- $\alpha$  and MCP-1 contents were measured by ELISA Kits (Jianglai Biotechnology Co. LTD, Shanghai, China) according to product specifications.

## RNA Isolation and qRT-PCR

The TRIZOL reagent (Invitrogen, CA) was used to isolated total RNA according to product specifications. The concentration and purity of RNA were determined by NanoDrop2000 spectrophotometer (Thermo Fisher Scientific, MA). One microgram of RNA was reversed transcriptase to produce cDNA. qRT-PCR was performed using the CFX96 real-time PCR system (Bio-Rad, CA) with SYBR Premix Ex Taq™ II (Takara, Japan). The primer sequences: Mouse IL-1 $\beta$ : F 5'-GCCTCGTGC TGTCGGACCCATAT-3', R 5'-TCCTTTGAGGCCC AAGGCCACA-3'; Mouse TNF- $\alpha$ : F 5'-CATCTTCTCAA AATTCGAGTGACAA-3', R 5'-TGGGAGTAGACA AGGTACAACCC-3'; Mouse MCP-1: F 5'-CTTC TGGGCTGCTGTTCA-3', R 5'-CCAGCCTA CTCATTGGGATCA-3'; Mouse  $\beta$ -actin: F 5'-CATT GCTGACAGGATGCAGAA-3', R 5'-AT GGTGC TAGGAGCCAGAAGC-3'; Human IL-1 $\beta$ : F 5'-ATGAT GGCTTATTACAGTGGCAA-3', R 5'-GTCCGAGAT TCGTAGCTGGA-3'; Human TNF- $\alpha$ : F 5'-TCAAT CGGCCCGACTATCTC-3', R 5'-ATGTTTCGTCCTC

CTCACAGG-3'; Human  $\beta$ -actin: F 5'-CCCTGG AGAAGAGCTACGAG-3', R 5'-GGAAGGAAGGC TGGAAAGAGT-3'.

## Western Blot

The cell extract and fragments of renal tissue were obtained by using lysis buffer (Beyotime, Jiangsu, China), and then protein concentration to be detected by BCA kit (Beyotime, Jiangsu, China). Ten percent SDS-PAGE gels were used to separate proteins, and then transferred to nitrocellulose membrane. The membranes were sealed with blocking buffer containing 5% skimmed milk at 37°C for 1 h and incubated with the corresponding first antibodies overnight at 4°C. After incubation with HRP-conjugated secondary antibody for 45 min at 37°C, the bands were detected with ECL developer.

## Immunofluorescence Assay

HK-2 cells were grown on glass coverslips and then treated with HG, which were either pre-treated or not pre-treated with wogonin for 24 h. HK-2 cells were fixed in 4% paraformaldehyde for 10 min, and sealed with 10% BSA (bovine serum albumin). Subsequently, the primary antibodies were incubated overnight. The cells were then incubated with the FITC-conjugated donkey anti-rabbit IgG, and incubated with DAPI for 5 min to stain the nuclei. Finally, slides were examined by using a fluorescence microscope (Zeiss Spot; Carl Zeiss Canada Ltd, Canada).

## Molecular Docking

The potential interactions between wogonin and PI3K were studied by molecular docking. Discovery Studio 2017 R2 (BIOVIA Software, Inc., San Diego, CA, United States) software was employed in this study. The structure of wogonin was optimized by Minimize protocol. Co-crystallized structure of PI3K (PDB ID: 1E7V) was downloaded from the RCSB Protein Data Bank. PI3K was prepared by Prepare protein protocol. The use of CDOCKER protocol was to molecular docking. Other parameters were set to default values.

## CETSA

HK-2 cells were cultured with or without wogonin for 24 h. After that, cellular proteins were extracted by using RIPA buffer. Adjust the sample to a similar concentration according to the BCA results. Each sample was allocated into multiple PCR tubes and processed at different temperatures

for 10 min on a PCR thermal cycler (Eppendorf, Germany). These proteins were then examined by Western blot.

## Statistical Analyses

All experiments were conducted independently for 3 times. Data were presented as the mean  $\pm$  standard deviation (SD). Statistical significance of differences were confirmed by student's two-tailed *t*-test or one-way ANOVA using GraphPad Prism 5 software.  $P < 0.05$  was regarded as statistically remarkable.

## Results

### Wogonin Alleviates Renal Injury in STZ-Induced Diabetic Mice

The molecular structure of wogonin is shown in [Figure 1A](#). To test the effect of wogonin in diabetic mice, diabetic mice were received wogonin (10, 20, 40 mg/kg). In our data, kidney/body weight, blood glucose, CRE, BUN and 24 h urine albumin levels in DM group were higher than those in NC group. After treatment with wogonin, there was no available difference in blood glucose level between DM group and DM+Wog groups. However, the other three indexes were markedly reduced by wogonin treatment in DM+Wog groups, indicating that wogonin treatment protected kidney from damage ([Figure 1B–F](#)). In the result of PAS staining, we found that wogonin treatment attenuated the glomerular mesangial expansion index and tubulointerstitial injury index in STZ-induced diabetic mice ([Figure 1G–I](#)). Moreover, result from Western blot showed that level of KIM-1 in diabetic mice was increased, and wogonin suppressed level of KIM-1 in a dose-dependent manner ([Figure 1J](#)).

### Wogonin Attenuates Inflammation and Autophagic Dysfunction in STZ-Induced Diabetic Mice

In the current study, we found wogonin had anti-inflammatory effect on diabetic mice and immunohistochemistry data found that wogonin reduced the level of TNF- $\alpha$  ([Figure 2A](#)). The mRNA levels of IL-1 $\beta$ , TNF- $\alpha$  and MCP-1 were dramatically up-regulated in diabetic mice ([Figure 2B](#)), and after treatment with wogonin, these cytokines were decreased. To demonstrate the change of autophagy under diabetic pathological stress, we found that autophagy-related proteins were enriched after treatment with wogonin. The results from Western blot showed that autophagy-related proteins such as LC3, Beclin1, and Atg7 were markedly decreased in diabetic mice, and wogonin enhanced the

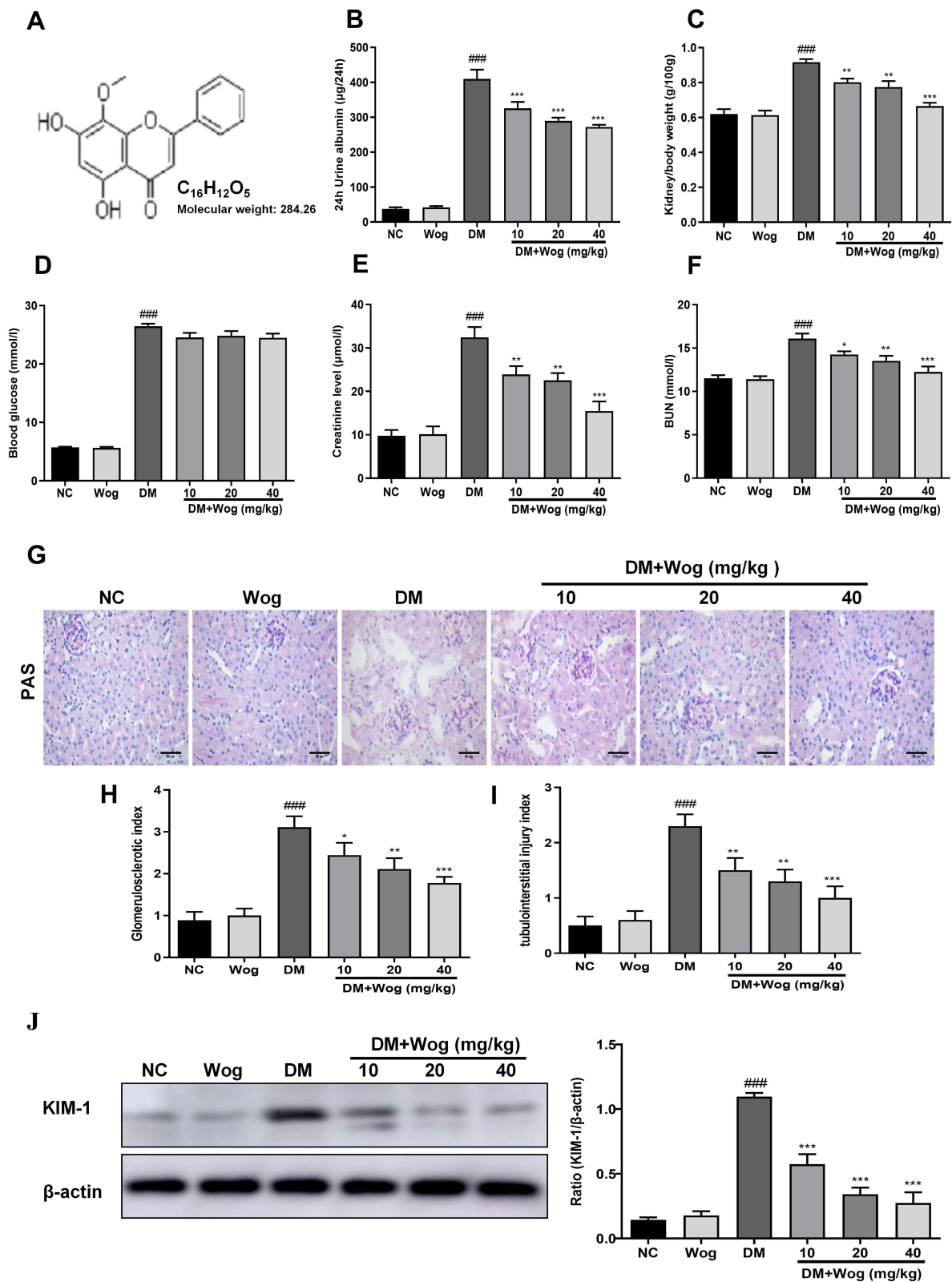


**Figure 1** Primary metabolic parameters and kidney injury in diabetic mice. **(A)** The molecular structural formula of wogonin. **(B)** Analysis of urine albumin excretion. **(C)** Kidney/body weight. **(D)** Blood glucose. **(E)** Serum creatinine assay. **(F)** Serum BUN assay. **(G)** Histological observations of renal sections stained with PAS. **(H)** Glomerulosclerotic index. **(I)** Tubulointerstitial injury index. **(J)** The protein expression level of KIM-1 in mice renal tissues. Results represent means  $\pm$  SEM for 6–8 mice. ### $p < 0.001$  VS NC. \* $p < 0.05$ , \*\* $p < 0.01$ , \*\*\* $p < 0.001$  VS DM. Scale bar = 50 $\mu$ m.

**Abbreviations:** BUN, blood urea nitrogen; CRE, creatinine; DM, diabetes mellitus; KIM-1, kidney injury molecule I; NC, normal control; PAS, periodic acid–Schiff; Wog, wogonin.

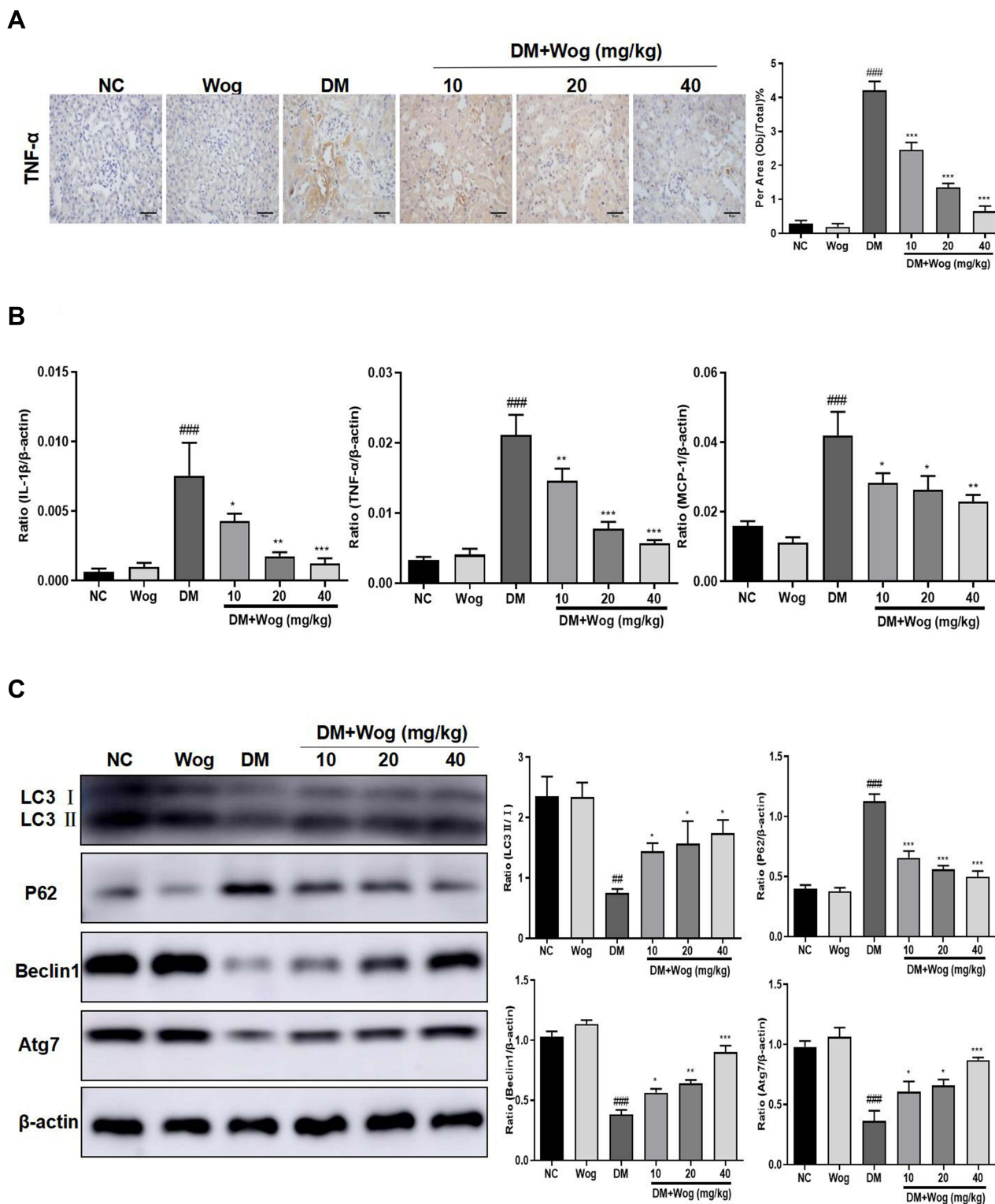


**Figure 2** Wogonin attenuates renal inflammation and autophagic dysfunction in diabetic mice. **(A)** Immunohistochemistry of TNF- $\alpha$  in mice kidney. **(B)** Real-time PCR of IL-1 $\beta$ , TNF- $\alpha$ , and MCP-1 in mice kidney. **(C)** Western blot analysis of LC3, P62, Beclin1 and Atg7 in mice kidney. Results represent means  $\pm$  SEM for 6–8 mice. ### $p$  < 0.01, #### $p$  < 0.001 VS NC. \* $p$  < 0.05, \*\* $p$  < 0.01, \*\*\* $p$  < 0.001 VS DM. Scale bar = 50 $\mu$ m.

**Abbreviations:** DM, diabetic mellitus; IL-1 $\beta$ , interleukin-1 $\beta$ ; MCP-1, mononuclear chemotactic protein-1; NC, normal control; TNF- $\alpha$ , tumor necrosis factor- $\alpha$ ; Wog, wogonin.

induction. Western blot analysis also showed that P62 widely used to monitor autophagic activity was up-regulated in diabetic mice, and wogonin inhibited P62 expression (Figure 2C).

### Wogonin Ameliorates Fibrosis in STZ-Induced Diabetic Mice

It was well known that the accumulation of ECM was an essential pathological feature of tubulointerstitial fibrosis. By Masson staining, we found that collagen deposition in STZ-induced diabetic mice were significantly up-regulated, while wogonin-treated was markedly reduced (Figure 3A). Meanwhile, wogonin reduced the expression of Col-I, FN and  $\alpha$ -SMA. Moreover, loss of E-cadherin staining was observed in diabetic mice, suggesting that epithelial adhesion perhaps disrupted, while wogonin treatment attenuated the inhibition (Figure 3B). Consistent with these notions, Western blot also confirmed the results (Figure 3C).

### Wogonin Induces Autophagy via the Inhibition of PI3K/Akt/mTOR Signaling Pathway in STZ-Induced Diabetic Mice

The PI3K/Akt/mTOR signaling pathway is known to regulate the autophagic processes. We used Western blot to analyze the effect of wogonin treatment on this pathway. Treatment with wogonin in diabetic mice leads to dose-dependent decreases in the levels of p-PI3K, p-Akt and p-mTOR (Figure 4).

### Wogonin Inhibits Inflammation via the Inhibition of NF- $\kappa$ B Signaling Pathway in STZ-Induced Diabetic Mice

Therefore, we evaluated the role of NF- $\kappa$ B signaling pathway in diabetic mice. Western blot results showed that the phosphorylation level of NF- $\kappa$ B p65 was increased in the renal tissues of diabetic mice and was suppressed in tissues of wogonin treated (Figure 4).

### Wogonin Attenuates HG-Induced Tubular Epithelial Cells Injury

To detect the effect of cell viability, HK-2 cells were treated with different concentrations of wogonin. The results in Figure 5A showed that concentration of wogonin was less than 16  $\mu$ M restored the viability of HG-treated cells. In addition, we evaluated the effect of wogonin by detecting level of KIM-1. Result showed that KIM-1 was

significantly down-regulated by effect of wogonin in a dose-dependent manner (2, 4, 8  $\mu$ M) (Figure 5B).

### Wogonin Attenuates Inflammation and Autophagic Dysfunction in HG-Induced Tubular Epithelial Cells

The gene expressions of the salient pro-inflammatory cytokines, IL-1 $\beta$  and TNF- $\alpha$  were increased in tubular epithelial cells, and wogonin markedly reduced inflammatory cytokines (Figure 5C). In addition, ELISA analysis suggested that wogonin decreased levels of inflammatory markers, such as IL-1 $\beta$ , TNF- $\alpha$ , and MCP-1 (Figure 5D). The levels of autophagy-related proteins LC3, Beclin1, and Atg7 were decreased and P62 was up-regulated in HG-induced cells, and wogonin reversed these phenomena (Figure 6A). By transmission electron microscopy, autophagic vacuoles commonly noted in HK-2 cells, were barely observed in HG-induced cells and markedly reinstated by wogonin treatment (Figure 6B).

### Wogonin Suppresses the HG-Induced ECM Accumulation

To detect the role of wogonin, HK-2 cells were exposed to 30 mM glucose to induce DN cell model. Results revealed that levels of ECM proteins such as Col-I, FN and  $\alpha$ -SMA were augmented in HG-induced cells. The reduction of E-cadherin, a specific epithelial cell marker, has been shown in HG-induced cells, and after wogonin treatment level of E-cadherin was up-regulated (Figure 7A). Similarly, this was consistently in favor of result from IF of  $\alpha$ -SMA (Figure 7B). These results indicated that wogonin suppressed EMT progression.

### Wogonin Induces Autophagy via the Inhibition of PI3K/Akt/mTOR Signaling Pathway in HG-Induced Tubular Epithelial Cells

The PI3K/Akt/mTOR signaling pathway is one of the crucial pathways regulating autophagy. We measured the effects of HG on PI3K/Akt/mTOR signaling pathways in HK-2 cells. The expressions of the phosphorylation of PI3K, Akt, mTOR were examined by Western blot analysis. Exposure of HK-2 cells to HG leads to significantly enhanced expressions of the phosphorylation of PI3K, Akt, mTOR. Treatment with wogonin suppressed HG-induced upregulation of p-PI3K and activation of Akt, mTOR in HK-2 cells (Figure 8).

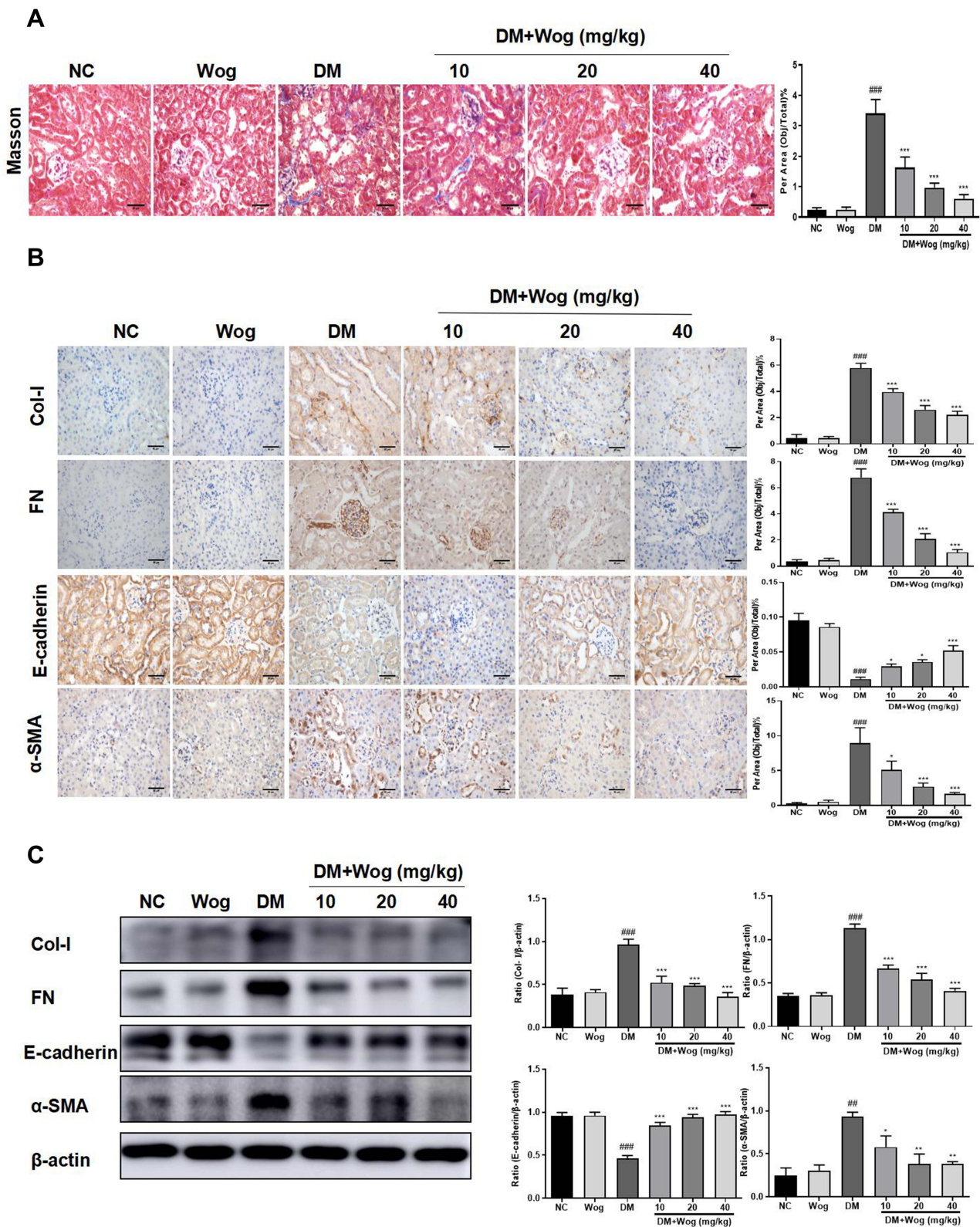


**Figure 3** Wogonin attenuates renal fibrosis in diabetic mice. **(A)** Masson staining and score of severity. **(B)** Immunohistochemistry of Col-I, FN, E-cadherin and α-SMA in mice kidney. **(C)** Western blot analysis of Col-I, FN, E-cadherin and α-SMA in mice kidney. Results represent means ± SEM for 6–8 mice. ### *p* < 0.01, #### *p* < 0.001 VS NC. \**p* < 0.05, \*\**p* < 0.01, \*\*\**p* < 0.001 VS DM. Scale bar = 50μm.

**Abbreviations:** α-SMA, α-smooth muscle actin; Col-I: collagen I; DM, diabetic mellitus; FN, fibronectin; NC, normal control; Wog, wogonin.



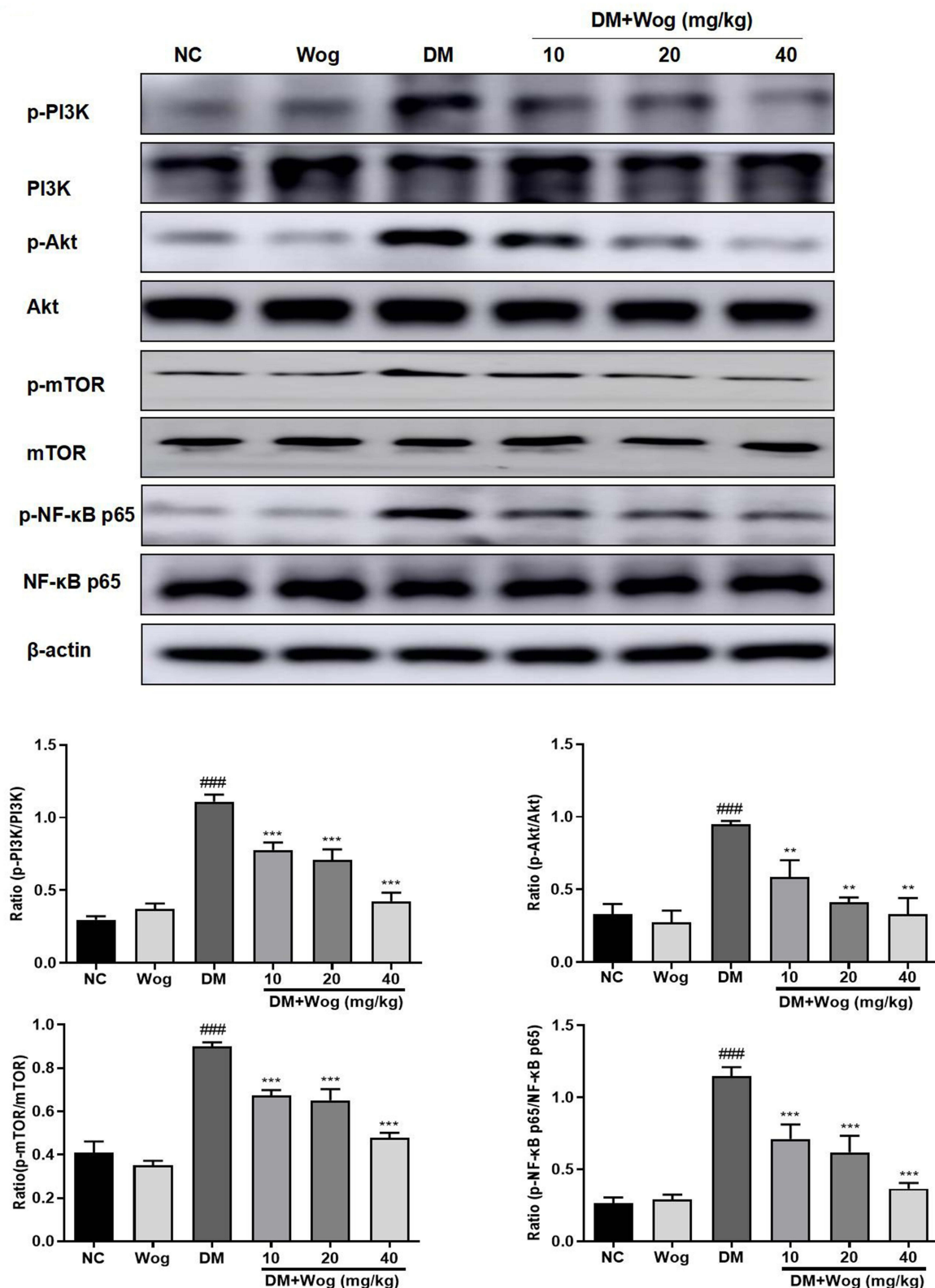


**Figure 4** Wogonin inhibits PI3K/Akt/ NF-κB Signaling pathway in diabetic mice. Western blot analysis of p-PI3K, p-Akt, p-mTOR, p-NF-κB p65 protein levels in kidney mice. Results represent means  $\pm$  SEM for 6–8 mice. ### $p < 0.001$  VS NC. \*\* $p < 0.01$ , \*\*\* $p < 0.001$  VS DM.

**Abbreviations:** Akt, protein kinase B; DM, diabetes mellitus; mTOR, mammalian target of rapamycin; NC, normal control; PI3K, phosphoinositide 3-kinase; Wog, wogonin.

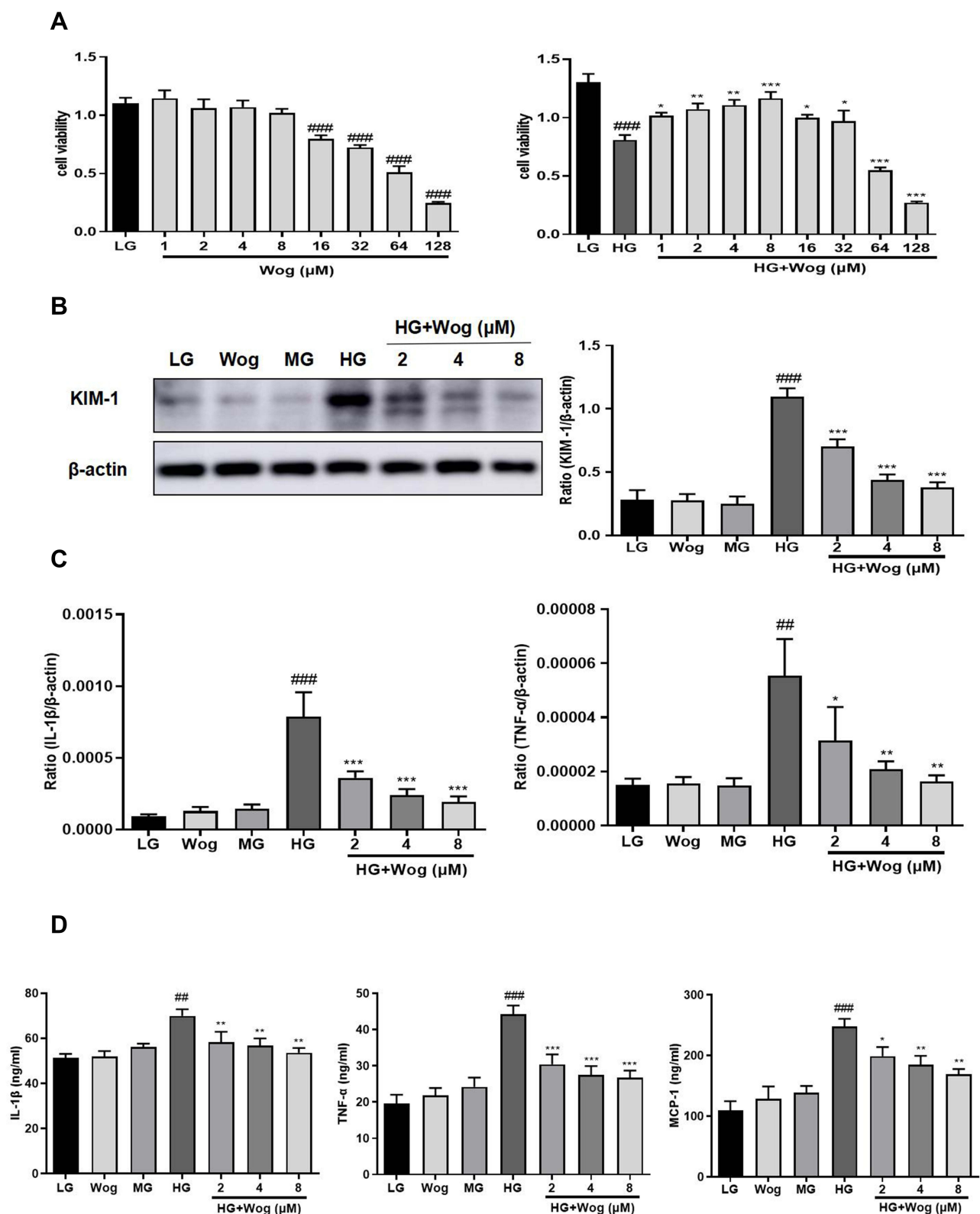
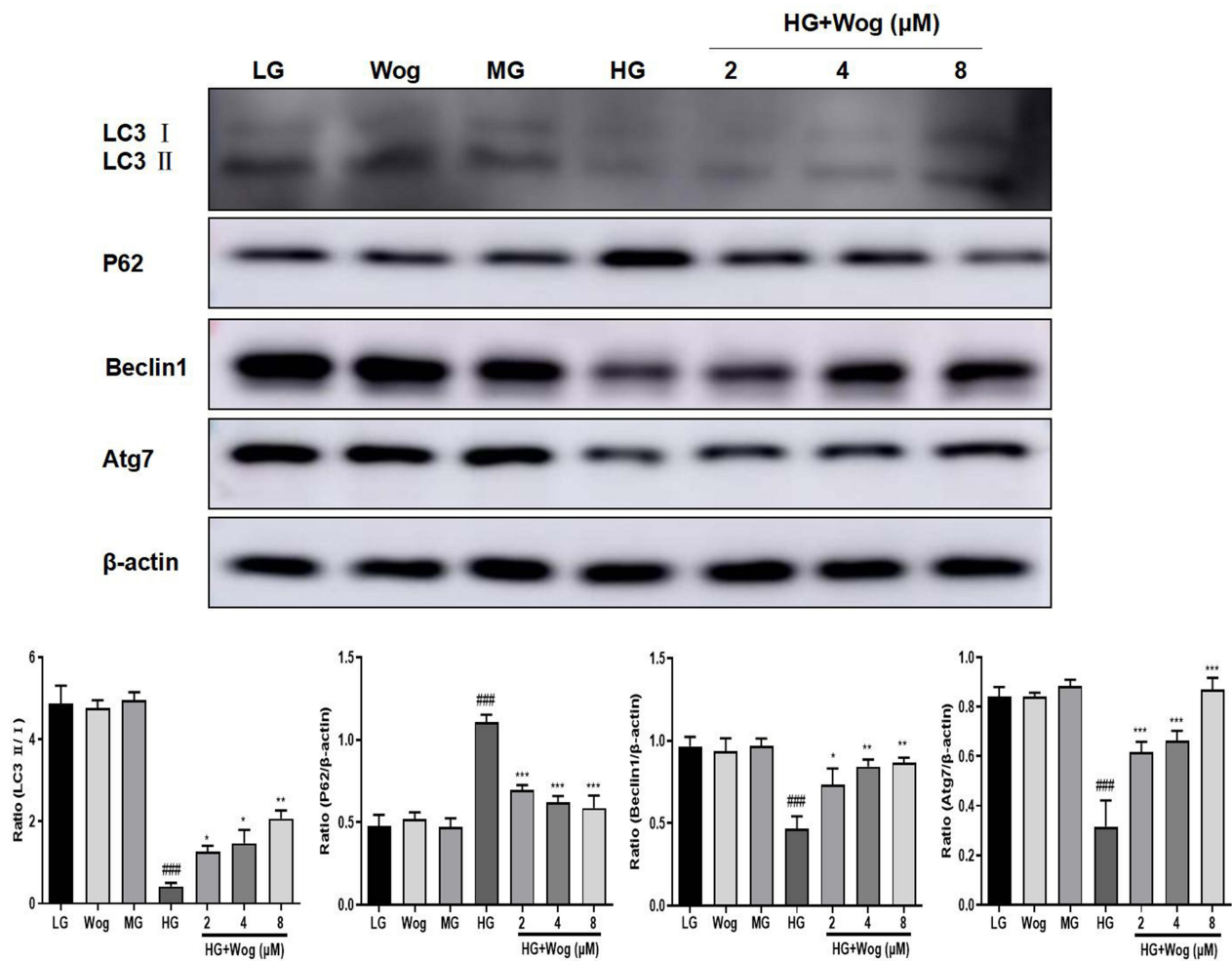


**Figure 5** Wogonin attenuates inflammation in HG-treated HK-2 cells. **(A)** MTT assay of wogonin on HK-2 cells viability and HG-treated HK-2 cells viability. **(B)** Western blot analysis of KIM-1 in HK-2 cells. **(C)** Real-time PCR of IL-1β and TNF-α in HK-2 cells. **(D)** ELISA of IL-1β, TNF-α and MCP-1 in HK-2 cells. Results represent means ± SEM for three independent experiments. ###*p* < 0.01, ####*p* < 0.001 VS LG. \**p* < 0.05, \*\**p* < 0.01, \*\*\**p* < 0.001 VS HG.

**Abbreviations:** HG, high glucose; IL-1β, interleukin-1β; KIM-1, kidney injury molecule 1; LG, low glucose; MG, mannitol glucose; TNF-α, tumor necrosis factor-α; Wog, wogonin.

A



B

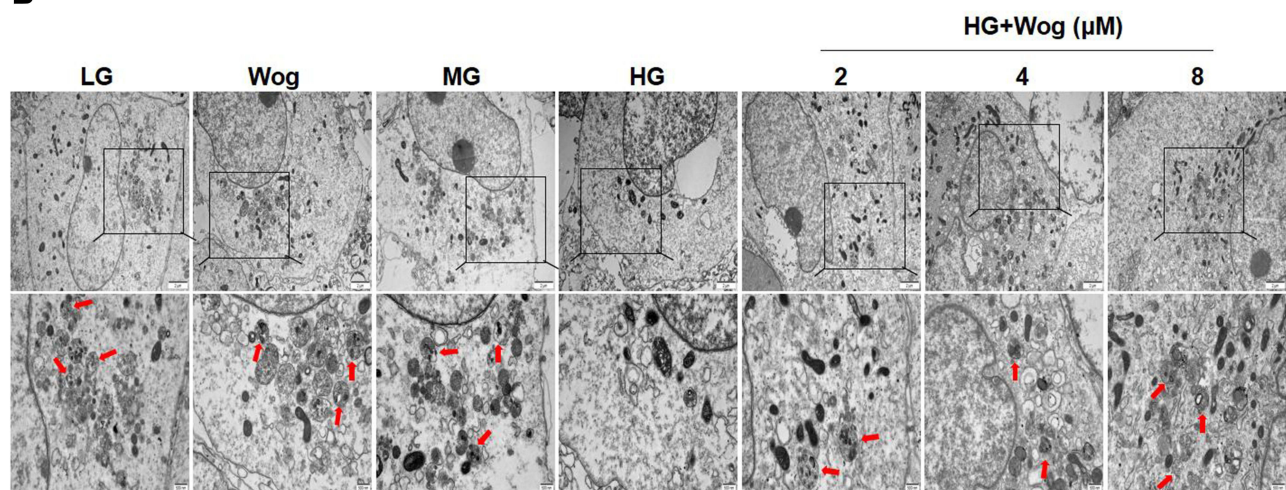
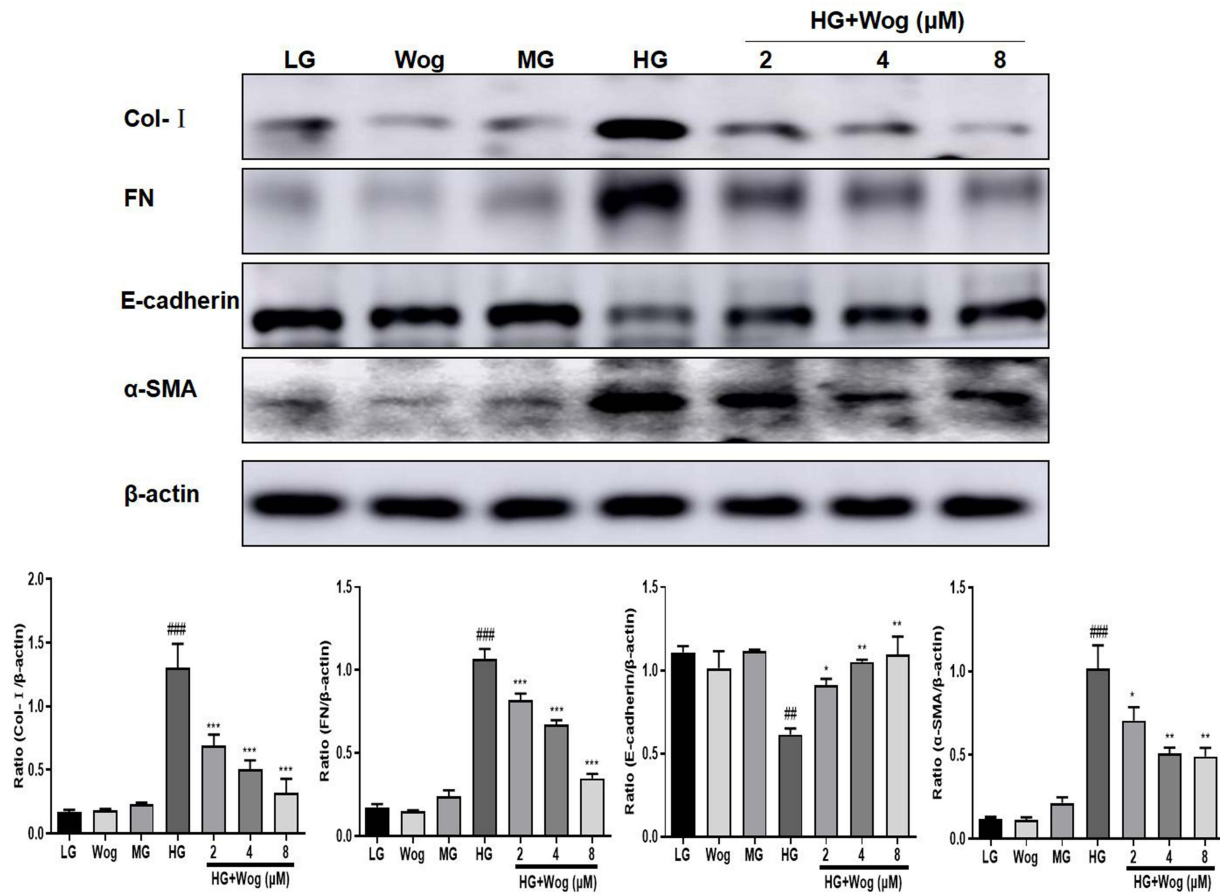


**Figure 6** Wogonin attenuates autophagic dysfunction in HG-treated HK-2 cells. **(A)** Western blot analysis of LC3, P62, Beclin1 and Atg7 and in HK-2 cells. **(B)** Representative transmission electron microscopy of autophagosome in HK-2 cells. In the enlarged view of the boxed area, autophagic vacuoles (red arrowhead indicate autolysosome), Scale bar = 500nm. Results represent means  $\pm$  SEM for three independent experiments. ####  $p < 0.001$  VS LG. \* $p < 0.05$ , \*\* $p < 0.01$ , \*\*\* $p < 0.001$  VS HG. **Abbreviations:** HG, high glucose; LG, low glucose; MG, mannitol glucose; Wog, wogonin.

**A**



**B**

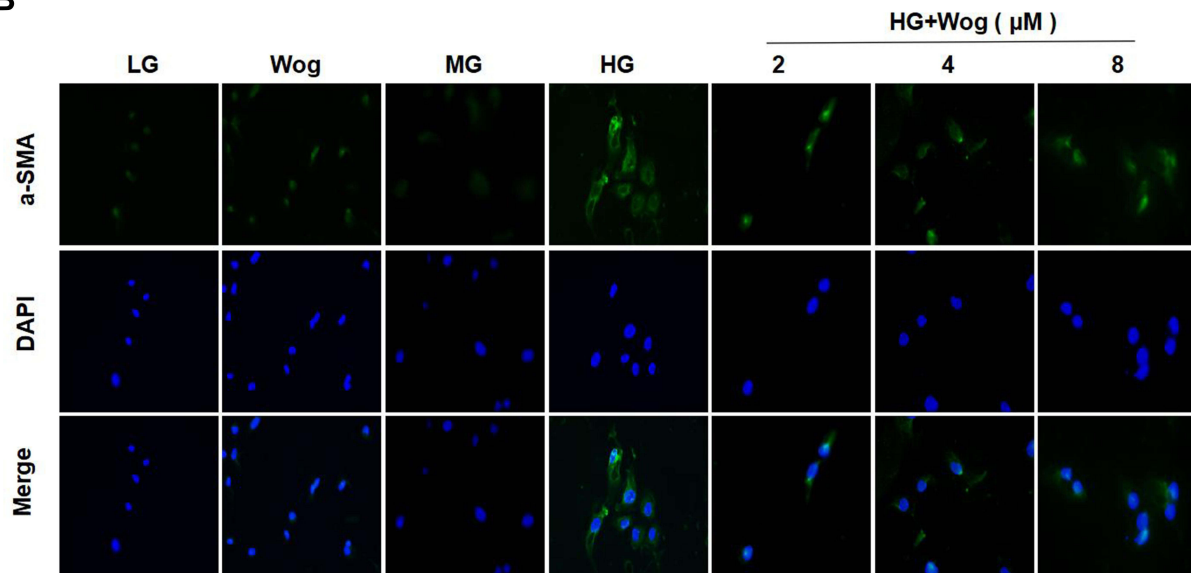


**Figure 7** Wogonin reduces the ECM in HG-treated HK-2 cells. **(A)** Western blot analysis of Col-I, FN, E-cadherin and  $\alpha$ -SMA in HK-2 cells. **(B)** IF of  $\alpha$ -SMA (green). Nuclei were counterstained with DAPI (blue). Results represent means  $\pm$  SEM for three independent experiments.  $###p < 0.01$ ,  $####p < 0.001$  VS LG.  $*p < 0.05$ ,  $**p < 0.01$ ,  $***p < 0.001$  VS HG.

**Abbreviations:**  $\alpha$ -SMA,  $\alpha$ -smooth muscle actin; Col-I, collagen I; ECM, extracellular matrix; FN, fibronectin; HG, high glucose; IF, immunofluorescence; LG, low glucose; MG, mannitol glucose; Wog, wogonin.

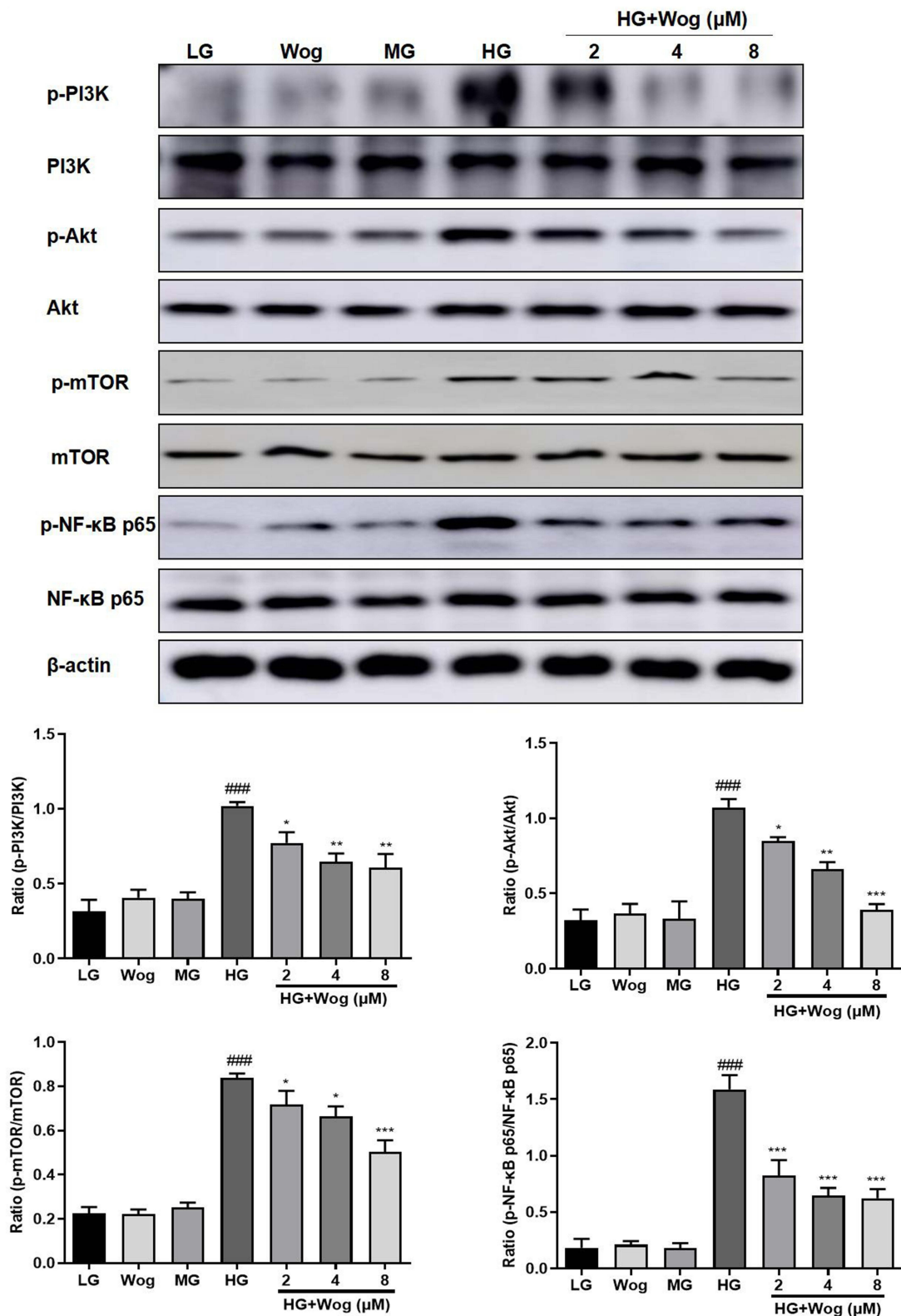


**Figure 8** Wogonin inhibits PI3K/Akt/NF-κB pathway in HG-treated HK-2 cells. Western blot analysis of p-PI3K, p-Akt, p-mTOR, p-NF-κB p65 protein levels in HK-2 cells. Results represent means  $\pm$  SEM for three independent experiments. ### $p < 0.001$  VS LG. \* $p < 0.05$ , \*\* $p < 0.01$ , \*\*\* $p < 0.001$  VS HG.

**Abbreviations:** Akt, protein kinase B; HG, high glucose; LG, low glucose. MG, mannitol glucose; mTOR, mammalian target of rapamycin; PI3K, phosphoinositide 3-kinase; Wog, wogonin.

## Wogonin Inhibits Inflammation via the Inhibition of NF- $\kappa$ B Signaling Pathway in HG-Induced Tubular Epithelial Cells

The protein level of NF- $\kappa$ B signaling pathway was detected to explore the mechanism of wogonin in down-regulation of inflammatory response. Western blot results demonstrated that the phosphorylation of NF- $\kappa$ B p65 in the HG group was higher than that of the LG groups, while the wogonin treatment induced significant decreases in dose-dependent. Therefore, wogonin could be considered to inhibit inflammation (Figure 8).

## Wogonin May Bind to PI3K in HG-Induced Tubular Epithelial Cells

Just like with the protein kinases, the ATP binding site of PI3K is located in a cleft between the N- and the C-terminal lobes of the catalytic domain (Figure 9A). The structures showed that wogonin may bind with many interactions in this site of PI3K. The interactions in PI3K involved conventional hydrogen bond between the carbonyl of GLU880 and the -OH group of wogonin, carbon hydrogen bond between the carbonyl of VAL882 and -H of wogonin and other interactions, such as van der Waals, pi-alkyl, and pi-pi T-shaped, which contributed to the binding affinity of wogonin with PI3K. The docking energy value of the highest scoring position, evaluated by CDocker, was 36.2118 kcal/mol. All the results showed that wogonin makes more widespread interactions with this site than the ATP does.

To evaluate target engagement, we confirmed the interaction between wogonin and PI3K protein by CETSA. The results indicated that the denaturation temperature of PI3K differed in the range of 50°C–65°C with or without wogonin treated. Interestingly, after treated with wogonin, PI3K had significantly greater thermal stability in HK-2 cells. These results demonstrated that wogonin may bind to the PI3K protein to improve the thermal stability (Figure 9B).

## Wogonin Attenuates HG-Induced Autophagy, Inflammation, and ECM Accumulation Through PI3K-Dependent Mechanisms

First, the suitable concentration of PI3Ki concentration (10 $\mu$ M) used in the present study was determined by MTT (Figure 9C). Then, we inhibited the expression of PI3K by PI3Ki (Figure 10A). When PI3K was inhibited,

wogonin could not further suppress KIM-1, autophagy-related protein levels and pro-inflammatory cytokines (Figure 10B–D). Meanwhile, we found that wogonin could not inhibit the accumulation of ECM after PI3K was inhibited, suggesting that wogonin mainly plays a role by targeting PI3K (Figure 11A). Importantly, results showed that inhibition of PI3K could decrease HG-induced Akt phosphorylation and mTOR mediated autophagy response significantly. Moreover, results showed that inhibition of PI3K expression could decrease HG-induced NF- $\kappa$ B mediated inflammatory response (Figure 11B). That was to say, in the case of PI3K inhibited, wogonin was unable to play its cellular protective role.

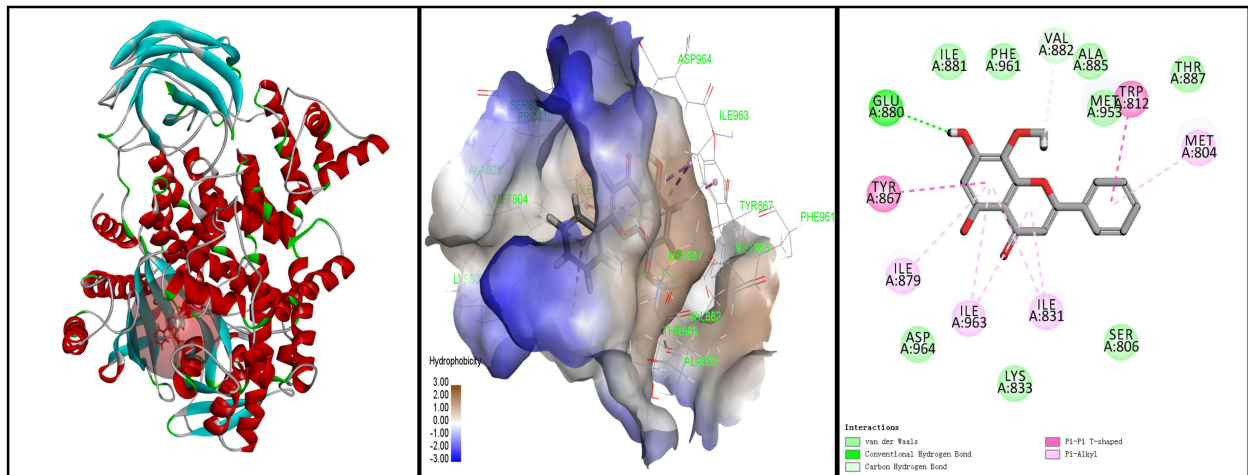
## Discussion

DN is a chronic renal disease characterized by progressive renal fibrosis. Renal interstitial fibrosis reflecting the degree of kidney damage was better than glomerulosclerosis, is one of the important pathological bases of DN.<sup>2</sup> Thereby, it is necessary to make sense the pathogenesis of DN and look for a new therapy. Our laboratory found that wogonin could reduce glomerular sclerosis, urinary albumin, and tubular epithelial cell injury in vivo. We also found that wogonin down-regulated the level of pro-inflammatory cytokines and autophagic dysfunction in vivo and in vitro. The mechanism was that wogonin reduced renal tubular inflammatory response and autophagic dysfunction to decrease of the expression of ECM proteins by targeting PI3K.

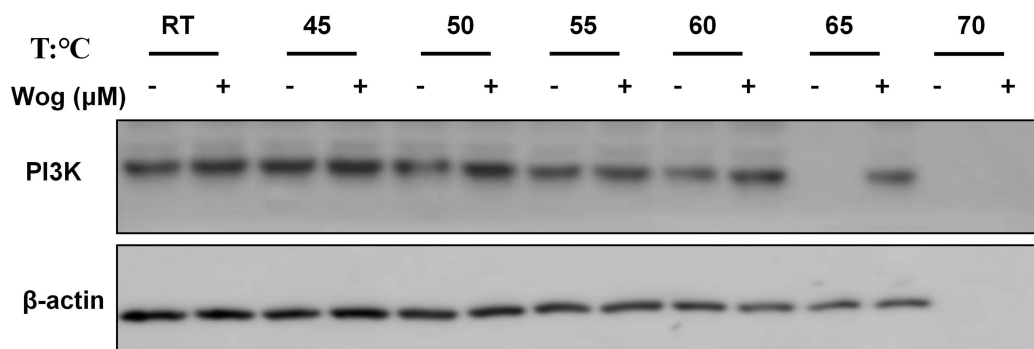
Wogonin is a kind of flavonoids, which has many pharmacological effects, such as anti-oxidation, anti-inflammatory and anti-fibrosis.<sup>8–10</sup> Wogonin inhibits the proliferation of HG-treated mesangial cells.<sup>11</sup> Wogonin inhibits H<sub>2</sub>O<sub>2</sub>-induced angiogenesis via suppressing PI3K/Akt/NF- $\kappa$ B pathway.<sup>28</sup> In order to better understand the effects of wogonin, our laboratory tested biochemical indices in diabetic mice. The results confirmed that wogonin reduced urinary albumin, CRE and BUN in dose-dependently, but did not reduce the level of blood glucose compared with diabetic mice. In stark contrast, kidneys from mice treated with wogonin exhibited lessened renal tubular lesions in a dose-dependent mode.

Our study confirmed that HG condition was suitable for producing pro-inflammatory cytokines, IL-1 $\beta$ , TNF- $\alpha$ , and MCP-1, which play critical roles in DN. Wogonin inhibited HG-induced production of these inflammatory cytokines in vivo and in vitro. More and more studies have confirmed that DN is a micro-inflammatory disease,

A



B



C

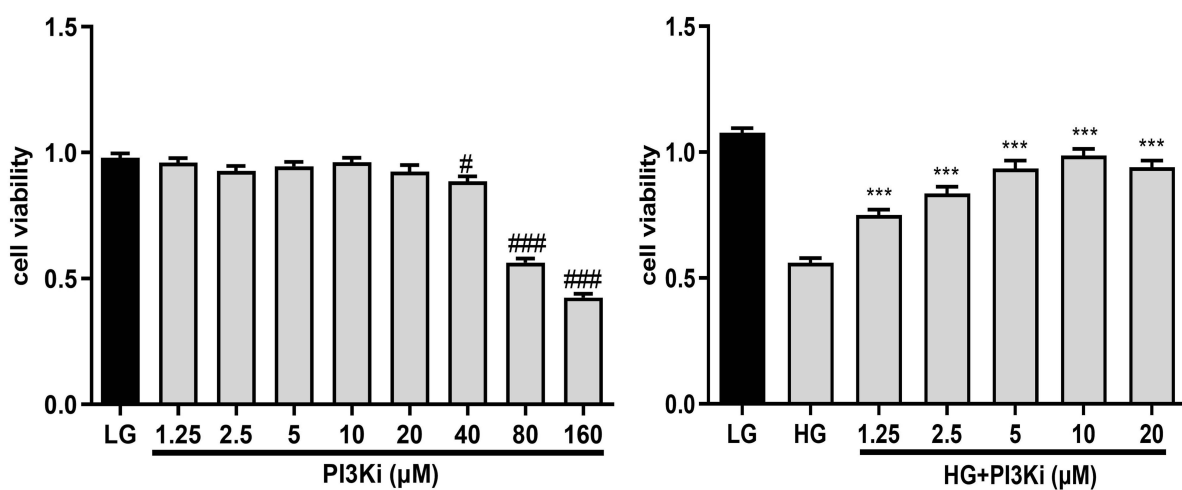


**Figure 9** Wogonin may bind to PI3K in HG-treated HK-2 cells. **(A)** Co-crystallized structure of PI3K (PDB ID: 1E7V) was downloaded from the RCSB Protein Data Bank. **(B)** CETSA analysis of HK-2 cells. **(C)** MTT assay of PI3Ki in HK-2 cells viability. Results represent means  $\pm$  SEM for three independent experiments. # $p < 0.05$ , ### $p < 0.001$  VS LG. \*\*\* $p < 0.001$  VS HG.

**Abbreviations:** CETSA, Cellular Thermal Shift Assay; HG, high glucose; PI3K, phosphoinositide 3-kinase; PI3Ki, PI3K inhibitor; Wog, wogonin.

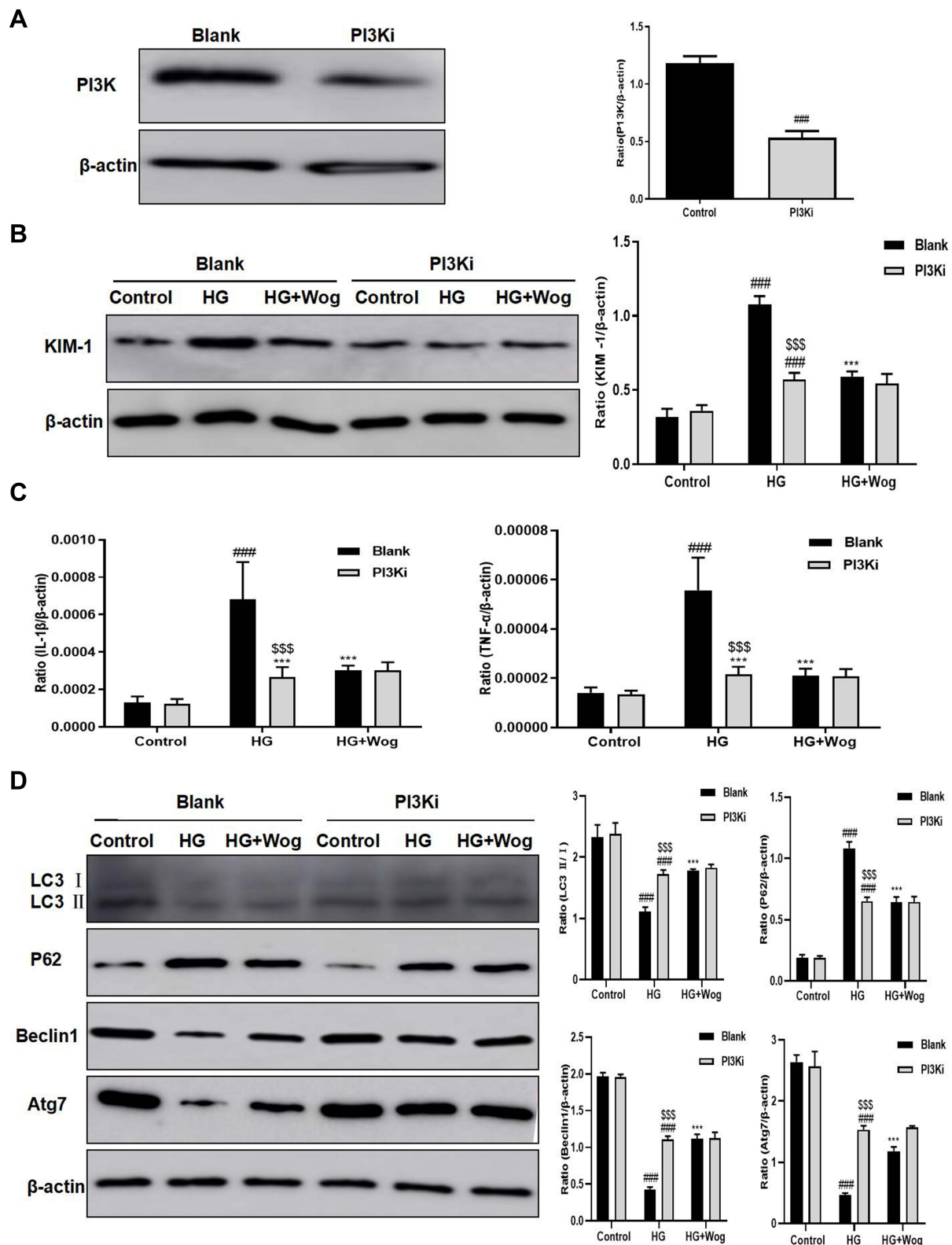


**Figure 10** Wogonin fails to reduce the HG-induced cells inflammatory response and autophagy dysfunction in PI3K-inhibited HK-2 cells. **(A)** Western blot of PI3K in HK-2 cells. **(B)** Western blot of KIM-1 in HK-2 cells. **(C)** Real-time PCR of IL-1 $\beta$  and TNF- $\alpha$  in HK-2 cells. **(D)** Western blot analysis of LC3, P62, Beclin1 and Atg7 and in HK-2 cells. Results represent means  $\pm$  SEM for three independent experiments. <sup>###</sup>*p* < 0.001 VS Control. <sup>\*\*\*</sup>*p* < 0.001 VS HG. <sup>\$\$\$</sup>*p* < 0.001 VS Blank.

**Abbreviations:** HG, high glucose; IL-1 $\beta$ , interleukin-1 $\beta$ ; KIM-1, kidney injury molecule 1; PI3K, phosphoinositide 3-kinase; PI3Ki, PI3K inhibitor; TNF- $\alpha$ , tumor necrosis factor- $\alpha$ ; Wog, wogonin.



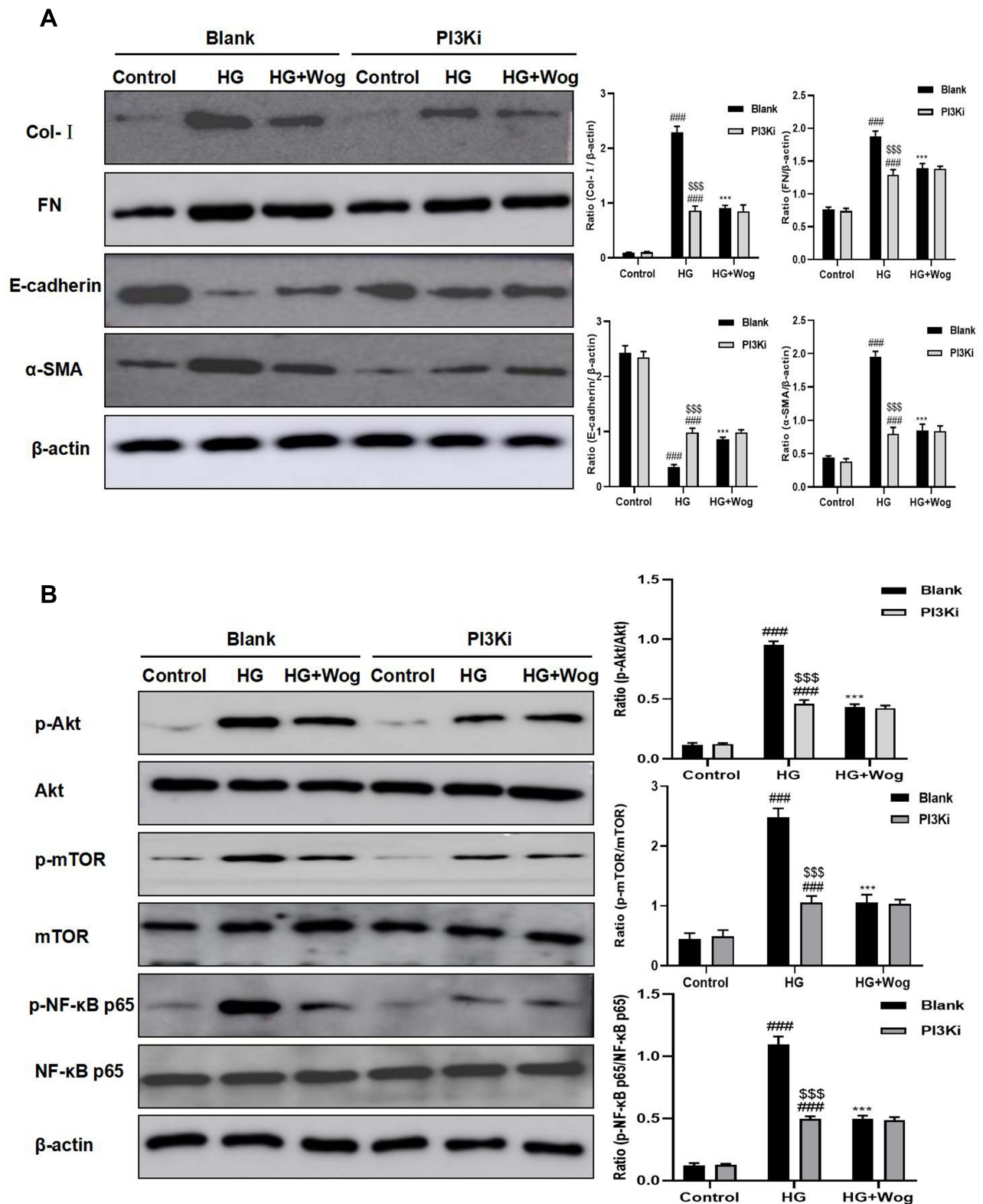


**Figure 11** Inhibited PI3K and treatment with wogonin have cellular protective role. **(A)** Western blot analysis of Col-1, FN, E-cadherin and  $\alpha$ -SMA in HK-2 cells. **(B)** Western blot analysis of p-Akt, p-mTOR, p-NF- $\kappa$ B p65 protein levels in HK-2 cells. Results represent means  $\pm$  SEM for three independent experiments. ####  $p < 0.001$  VS Control. \*\*\* $p < 0.001$  VS HG. \$\$\$ $p < 0.001$  VS Blank. **Abbreviations:** Akt, protein kinase B;  $\alpha$ -SMA,  $\alpha$ -smooth muscle actin; Col-1, collagen I; FN, fibronectin; HG, high glucose; mTOR, mammalian target of rapamycin; PI3K, phosphoinositide 3-kinase; PI3Ki, PI3K inhibitor; Wog, wogonin.

in which the structure of glomerulus and renal tubules is changed.<sup>13,29,30</sup> Recent studies have confirmed that HG induced the activation of NF- $\kappa$ B pathway through signal transducer, leading to accumulation of cytokines in the intrinsic cells of kidney, which can damage intrinsic cells of kidney and aggravate the procession of DN.<sup>31,32</sup>

Autophagy is an important mechanism to degrade cellular damaged organelles and protein aggregates to promote cell survival and maintain homeostasis.<sup>19</sup> Our laboratory has found that HG-inhibited expressions of LC3, Beclin1 and Atg7, at the same time induced expression of P62, suggesting that autophagy was dysfunction in tubular epithelial cells. However, wogonin increased the induction of autophagy. Thus, lack of autophagy may be deleterious. Study has found that renal tubular epithelial cells showed high expression of autophagy and autophagic dysfunction could induce renal tubular epithelial cell damage in vivo and in vitro.<sup>33,34</sup> Autophagy has the potential to suppress kidney damage from chronic inflammation.<sup>35</sup> Autophagy sustains cellular homeostasis through inactivation of inflammatory responses by regulating the degradation of NF- $\kappa$ B signaling components, thus terminating the activation of NF- $\kappa$ B.<sup>36–38</sup> Therefore, autophagy can regulate the inflammatory response to reduce the pathological changes of the kidney.

Through our experimental study, we found that Masson's trichrome staining showed increased accumulation of collagen fibers in diabetic mice. Meanwhile, PAS staining showed that glomerular mesangial expansion index and tubulointerstitial damage index were increased in diabetic mice. In this study, an immunohistochemical assay was used to identify the deposition of ECM proteins in tubulointerstitium, and wogonin could reverse these. Our study further corroborated that the action of wogonin reduced ECM accumulation in HG-induced HK-2 cells. DN is a chronic kidney disease characterized by progressive renal fibrosis, in which renal tubulointerstitial fibrosis is the main pathological feature and plays a vital role in the progression of DN.<sup>39</sup> The continuous decline of renal function is related to the excessive accumulation of ECM proteins.<sup>5</sup> Renal epithelial-to-mesenchymal transition (EMT) is the key linked of renal tubulointerstitial fibrosis.<sup>6</sup> A recent study showed that tubular epithelial cells can express fibroblast markers in DN, which contribute to the accumulation of tubulointerstitial and matrix proteins in DN.<sup>40</sup>

In vivo and in vitro experimental results indicated that wogonin effectively suppressed HG-induced inflammatory response and autophagic dysfunction by inhibiting the PI3K/Akt/NF- $\kappa$ B pathway. The structures found that wogonin

binds with many interactions in this site of PI3K. The interactions in PI3K involved conventional hydrogen bond between the carbonyl of GLU880 and the -OH group of wogonin, carbon hydrogen bond between the carbonyl of VAL882 and -H of wogonin and other interactions, such as van der Waals, pi-alkyl, and pi-pi T-shaped, which contributed to the binding affinity of wogonin with PI3K. The docking energy value of the highest scoring position, evaluated by CDOCKER, was 36.2118kcal/mol. Further, CETSA was used to confirm that wogonin may bind to PI3K with a high affinity. With PI3K inhibitor, wogonin did not further remission in HG-induced high levels of production of autophagic dysfunction and pro-inflammatory cytokines, which hinted that wogonin played a protective role by targeting PI3K. It has been reported that PI3K/Akt pathway plays a critical role in DN.<sup>41</sup> The mTOR, mainly mediated by PI3K/Akt signaling transduction, can negatively regulate autophagy.<sup>24</sup> In diabetic patients, a large amount of undissolved P62/SQSTM1 was detected in the proximal tubular epithelial cells, indicating that there is a lack of autophagy.<sup>27,42</sup> The protein is itself degraded by autophagy and may serve to link ubiquitinated proteins to the autophagic machinery to enable their degradation in the lysosome. Since P62 accumulates when autophagy is inhibited, and decreased level can be observed when autophagy is induced, P62 may be used as a marker to study autophagic flux.<sup>43</sup> Autophagy is responsible for the degradation of P62.<sup>44</sup> Thus, the destruction of autophagy is usually accompanied by a large accumulation of P62. Importantly, the autophagy cargo receptor P62, regulates NF- $\kappa$ B signaling activation.<sup>45</sup> NF- $\kappa$ B activation leads to increased release of pro-inflammatory cytokines and aggravates kidney damage.<sup>31,32</sup>

Taken together, our experiment firstly found that wogonin regulated autophagy and inflammation via targeting PI3K, the important connection point of PI3K/Akt/NF- $\kappa$ B signaling pathway reducing tubular injury in diabetic mice. However, it is still a need to further explore the pathogenesis of DN.

## Abbreviations

Akt, protein kinase B; BUN, blood urea nitrogen; CETSA, Cellular Thermal Shift Assay; CRE, creatinine; DN, diabetic nephropathy; DM, diabetic mellitus; ESRD, end-stage renal nephropathy; ECM, extracellular matrix; EMT, epithelial-to-mesenchymal transition; HK-2, human tubular epithelial cells; HG, high glucose; IF, immunofluorescence; IHC, immunohistochemistry; LG, low glucose; MG, mannitol glucose; mTOR, mammalian target of rapamycin; NC, normal control; PAS, Periodic acid-Schiff; PI3K,

phosphoinositide 3-kinase; PI3Ki, PI3K inhibitor; STZ, streptozotocin; Wog, wogonin.

## Data Sharing Statement

All the data in the manuscript are available upon reasonable request from the corresponding author.

## Author Contributions

All authors made substantial contributions to conception and design, acquisition of data, or analysis and interpretation of data; took part in drafting the article or revising it critically for important intellectual content; agreed to submit to the current journal; gave final approval of the version to be published; and agreed to be accountable for all aspects of the work.

## Funding

This study was supported by the Scientific Research Foundation of the Institute for Translational Medicine of Anhui Province (number: 2017zhyx01) and Natural Science Foundation of Anhui Province (No: 1808085MH236).

## Disclosure

All authors declare that there are no competing interests.

## References

- Kawanami D, Matoba K, Utsunomiya K. Signaling pathways in diabetic nephropathy. *Histol Histopathol.* 2016;31:1059–1067. doi:10.14670/HH-11-777
- Habib SL. Alterations in tubular epithelial cells in diabetic nephropathy. *J Nephrol.* 2013;26:865–869. doi:10.5301/jn.5000287
- Phillips AO, Steadman R. Diabetic nephropathy: the central role of renal proximal tubular cells in tubulointerstitial injury. *Histol Histopathol.* 2002;17:247–252. doi:10.14670/HH-17.247
- Louis K, Hertig A. How tubular epithelial cells dictate the rate of renal fibrogenesis? *World J Nephrol.* 2015;4:367–373. doi:10.5527/wjn.v4.i3.367
- Nangaku M. Mechanisms of tubulointerstitial injury in the kidney: final common pathways to end-stage renal failure. *Intern Med.* 2004;43:9–17. doi:10.2169/internalmedicine.43.9
- Li JP, Liu HJ, Takagi S, et al. Renal protective effects of empagliflozin via inhibition of EMT and aberrant glycolysis in proximal tubules. *JCI Insight.* 2020;5:e129034. doi:10.1172/jci.insight.129034
- Thomas MC, Burns WC, Cooper ME. Tubular changes in early diabetic nephropathy. *Adv Chronic Kidney Dis.* 2005;12:177–186. doi:10.1053/j.ackd.2005.01.008
- Du XS, Li HD, Yang XJ, et al. Wogonin attenuates liver fibrosis via regulating hepatic stellate cell activation and apoptosis. *Int Immunopharmacol.* 2019;75:105671. doi:10.1016/j.intimp.2019.05.056
- Khan NM, Haseeb A, Ansari MY, et al. Wogonin, a plant derived small molecule, exerts potent anti-inflammatory and chondroprotective effects through the activation of ROS/ERK/Nrf2 signaling pathways in human Osteoarthritis chondrocytes. *Free Radic Biol Med.* 2017;106:288–301. doi:10.1016/j.freeradbiomed.2017.02.041
- Meng XM, Ren GL, Gao L, et al. Anti-fibrotic effect of wogonin in renal tubular epithelial cells via Smad3-dependent mechanisms. *Eur J Pharmacol.* 2016;789:134–143. doi:10.1016/j.ejphar.2016.07.014
- Zheng ZC, Zhu W, Lei L, et al. Wogonin Ameliorates Renal Inflammation and Fibrosis by Inhibiting NF- $\kappa$ B and TGF- $\beta$ 1/Smad3 Signaling Pathways in Diabetic Nephropathy. *Drug Des Devel Ther.* 2020;14:4135–4148. doi:10.2147/DDDT.S274256
- Hong ZP, Wang LG, Wang HJ, et al. Wogonin exacerbates the cytotoxic effect of oxaliplatin by inducing nitrosative stress and autophagy in human gastric cancer cells. *Phytomedicine.* 2018;39:168–175. doi:10.1016/j.phymed.2017.12.019
- Yiu WH, Lin M, Tang SCW. Toll-like receptor activation: from renal inflammation to fibrosis. *Kidney Int Suppl.* 2014;4:20–25. doi:10.1038/kisup.2014.5
- Aghadavod E, Soleimani A, Amirani E, et al. Comparison Between Biomarkers of Kidney Injury, Inflammation, and Oxidative Stress in Patients with Diabetic Nephropathy and Type 2 Diabetes Mellitus. *Iran J Kidney Dis.* 2020;14:31–35.
- Moreno JA, Gomez-Guerrero C, Mas S, et al. Targeting inflammation in diabetic nephropathy: a tale of hope. *Expert Opin Inv Drug.* 2018;27:917–930. doi:10.1080/13543784.2018.1538352
- Salti T, Khazim K, Haddad R, et al. Glucose Induces IL-1 $\alpha$ -Dependent Inflammation and Extracellular Matrix Proteins Expression and Deposition in Renal Tubular Epithelial Cells in Diabetic Kidney Disease. *Front Immunol.* 2020;11:1270. doi:10.3389/fimmu.2020.01270
- Delanghe SE, Speeckaert MM, Segers H, et al. Soluble transferrin receptor in urine, a new biomarker for IgA nephropathy and Henoch-Schönlein purpura nephritis. *Clin Biochem.* 2013;46:591–597. doi:10.1016/j.clinbiochem.2013.01.017
- Lai KN, Leung JCK, Chan LYY, et al. Interaction between proximal tubular epithelial cells and infiltrating monocytes/T cells in the proteinuric state. *Kidney Int.* 2007;71(6):526–538. doi:10.1038/sj.ki.5002091
- Mizushima N, Levine B, Cuervo AM, Klionsk DJ. Autophagy fights disease through cellular self-digestion. *Nature.* 2008;451:1069–1075. doi:10.1038/nature06639
- Chen QH, Yu SL, Zhang K, et al. Exogenous H<sub>2</sub>S Inhibits Autophagy in Unilateral Ureteral Obstruction Mouse Renal Tubule Cells by Regulating the ROS-AMPK Signaling Pathway. *Cell Physiol Biochem.* 2018;49(6):2200–2213. doi:10.1159/000493824
- Du CY, Ren YZ, Yao F, et al. Sphingosine kinase 1 protects renal tubular epithelial cells from renal fibrosis via induction of autophagy. *Int J Biochem Cell Biol.* 2017;90:17–28. doi:10.1016/j.biocel.2017.07.011
- Yan Q, Song Y, Zhang L, et al. Autophagy activation contributes to lipid accumulation in tubular epithelial cells during kidney fibrosis. *Cell Death Discov.* 2018;4(1):2. doi:10.1038/s41420-018-0065-2
- Zhan XJ, Yan CX, Chen YB, et al. Celastrol antagonizes high glucose-evoked podocyte injury, inflammation and insulin resistance by restoring the HO-1-mediated autophagy pathway. *Mol Immunol.* 2018;104:61–68. doi:10.1016/j.molimm.2018.10.021
- Du CY, Zhang T, Xiao X, et al. Protease-activated receptor-2 promotes kidney tubular epithelial inflammation by inhibiting autophagy via the PI3K/Akt/mTOR signalling pathway. *Biochem J.* 2017;474(16):2733–2747. doi:10.1042/BCJ20170272
- Ding Y, Si K, Lee SY, et al. Autophagy regulates TGF- $\beta$  expression and suppresses kidney fibrosis induced by unilateral ureteral obstruction. *J Am Soc Nephrol.* 2014;25:2835–2846. doi:10.1681/ASN.2013101068
- Kim SI, Na HJ, Ding Y, et al. Autophagy promotes intracellular degradation of type I collagen induced by transforming growth factor (TGF)- $\beta$ 1. *J Biol Chem.* 2012;287:11677–11688. doi:10.1074/jbc.M111.308460
- Takahashi A, Takabatake Y, Kimura T, et al. Autophagy Inhibits the Accumulation of Advanced Glycation End Products by Promoting Lysosomal Biogenesis and Function in the Kidney Proximal Tubules. *Diabetes.* 2017;66(5):1359–1372. doi:10.2337/db16-0397

28. Zhou M, Song XM, Huang YJ, et al. Wogonin inhibits H<sub>2</sub>O<sub>2</sub>-induced angiogenesis via suppressing PI3K/Akt/NF-κB signaling pathway. *Vasc Pharmacol*. 2014;60:110–119. doi:10.1016/j.vph.2014.01.010
29. Chow FY, Nikolic-Paterson DJ, Ozols E, et al. Monocyte chemoattractant protein-1 promotes the development of diabetic renal injury in streptozotocin-treated mice. *Kidney Int*. 2006;69(1):73–80. doi:10.1038/sj.ki.5000014
30. Liu ZZ, Han YR, Zhao FC, et al. Nobiletin suppresses high-glucose-induced inflammation and ECM accumulation in human mesangial cells through STAT3/NF-κB pathway. *J Cell Biochem*. 2019;120:3467–3473. doi:10.1002/jcb.27621
31. Mezzano S, Aros C, Droguett A, et al. NF-κappaB activation and overexpression of regulated genes in human diabetic nephropathy. *Nephrol Dial Transpl*. 2004;19:2505–2512. doi:10.1093/ndt/gfh207
32. Sanz AB, Sanchez-Niño MD, Ramos AM, et al. NF-κappaB in renal inflammation. *J Am Soc Nephrol*. 2010;21:1254–1262. doi:10.1681/ASN.2010020218
33. Kimura T, Takabatake Y, Takahashi A, et al. Autophagy protects the proximal tubule from degeneration and acute ischemic injury. *J Am Soc Nephrol*. 2011;22:902–913. doi:10.1681/ASN.2010070705
34. Zhan M, Usman IM, Sun L, et al. Disruption of renal tubular mitochondrial quality control by Myo-inositol oxygenase in diabetic kidney disease. *J Am Soc Nephrol*. 2015;26:1304–1321. doi:10.1681/ASN.2014050457
35. Kimura T, Isaka Y, Yoshimori T. Autophagy and kidney inflammation. *Autophagy*. 2017;13:997–1003. doi:10.1080/15548627.2017.1309485
36. Agrawal V, Jaiswal MK, Mallers T, et al. Altered autophagic flux enhances inflammatory responses during inflammation-induced pre-term labor. *Sci Rep-UK*. 2015;5(1):9410. doi:10.1038/srep09410
37. Moscat J, Diaz-Meco MT. p62 at the crossroads of autophagy, apoptosis, and cancer. *Cell*. 2009;137(6):1001–1004. doi:10.1016/j.cell.2009.05.023
38. Trocoli A, Djavaheri-Mergny M. The complex interplay between autophagy and NF-κB signaling pathways in cancer cells. *Am J Cancer Res*. 2011;1:629–649.
39. Gewin LS. Renal fibrosis: primacy of the proximal tubule. *Matrix Biol*. 2018;68:248–262. doi:10.1016/j.matbio.2018.02.006
40. Zeng LF, Xiao Y, Sun L. A Glimpse of the Mechanisms Related to Renal Fibrosis in Diabetic Nephropathy. *Adv Exp Med Biol*. 2019;1165:49–79.
41. Qian X, He LL, Hao M, et al. YAP mediates the interaction between the Hippo and PI3K/Akt pathways in mesangial cell proliferation in diabetic nephropathy. *Acta Diabetol*. 2021;58(1):47–62. doi:10.1007/s00592-020-01582-w
42. Yang DY, Livingston MJ, Liu ZW, et al. Autophagy in diabetic kidney disease: regulation, pathological role and therapeutic potential. *Cell Mol Life Sci*. 2018;75:669–688.
43. Bjørkøy G, Lamark T, Pankiv S, et al. Monitoring autophagic degradation of p62/SQSTM1. *Method Enzymol*. 2009;452:181–197.
44. Katsuragi Y, Ichimura Y, Komatsu M. p62/SQSTM1 functions as a signaling hub and an autophagy adaptor. *FEBS J*. 2015;282(24):4672–4678. doi:10.1111/febs.13540
45. Chang CP, Su YC, Hu CW, et al. TLR2-dependent selective autophagy regulates NF-κB lysosomal degradation in hepatoma-derived M2 macrophage differentiation. *Cell Death Differ*. 2013;20:515–523. doi:10.1038/cdd.2012.146

## Drug Design, Development and Therapy

Dovepress

### Publish your work in this journal

Drug Design, Development and Therapy is an international, peer-reviewed open-access journal that spans the spectrum of drug design and development through to clinical applications. Clinical outcomes, patient safety, and programs for the development and effective, safe, and sustained use of medicines are a feature of the journal, which has also

been accepted for indexing on PubMed Central. The manuscript management system is completely online and includes a very quick and fair peer-review system, which is all easy to use. Visit <http://www.dovepress.com/testimonials.php> to read real quotes from published authors.

Submit your manuscript here: <https://www.dovepress.com/drug-design-development-and-therapy-journal>